ACS Sustainable Chemistry & Engineering

Research Article

Cite This: ACS Sustainable Chem. Eng. 2019, 7, 16690−16697

pubs.acs.org/journal/ascecg

Monosaccharide-Based Deep Eutectic Solvents for Developing Circularly Polarized Luminescent Materials

Liam VandenElzen and Todd A. Hopkins*

Department of Chemistry, Butler University, 4600 Sunset Avenue, Indianapolis, Indiana 46208, United States

Supporting Information

ABSTRACT: Deep eutectic solvents (DES) with chiral components can function as solvents in circularly polarized light-emitting materials. Deep eutectic solvents were developed with chiral hydrogen bond donors derived from biomass, glucose, and fructose, combined with tetrabutylammonium chloride ([TBA]Cl) as the hydrogen bond acceptor. Physical properties, such as density, melting points, relative polarity, and polarimetry, were measured for the monosaccharide-based DES. The impact of the [TBA]Cl:glucose ratio on the relative polarity is described. A racemic mixture of dissymmetric europium and terbium complexes is dissolved in the monosaccharide-based DES to measure the resulting chiral discrimination and induced circularly polarized luminescence (CPL). The samples showed red (Eu^{3+}) and green (Tb^{3+}) CPL with a sign that is controlled by the enantiomer (L vs D) of monosaccharide. Results from the glucose DES showed that the polarity of the DES and the anomeric form of the monosaccharide is important to the magnitude of induced CPL.

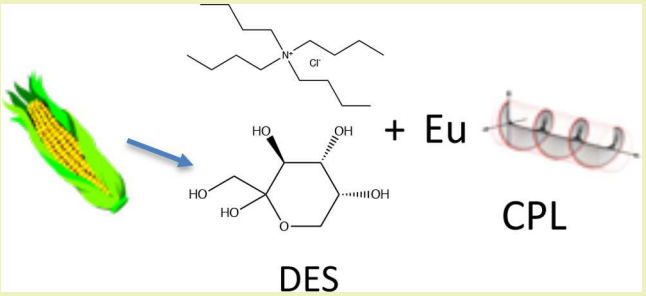

KEYWORDS: *Deep eutectic solvents, Circularly polarized luminescence, Europium, Terbium, Glucose, Fructose, Tetrabutylammonium chloride*

INTRODUCTION

Deep eutectic solvents (DES) have been studied as alternatives to molecular solvents and ionic liquids in many diverse applications, including, but not limited to, liquid−liquid extractions,[1−5] metal processing,[6] desulfurization of fuels,[7,8] and postconsumer waste recycling of rare earth elements.[9] Deep eutectic solvents are mixtures of Lewis acid(s) with Lewis base(s) that result in a melting point lower than the melting point of an ideal mixture of the components.[6,10,11] For many DES, the melting point depression is the result of hydrogen bonding between components, such as a mixture of an organic salt (e.g., ammonium salts) as the hydrogen bond acceptor (HBA) and an organic hydrogen bond donor (HBD). Deep eutectic solvents are often compared to ionic liquids (ILs) because they have similar physicochemical properties.[10] For potential applications, the most important property of DES may be the ability to control the physicochemical properties through the choice and molar ratio of HBA and HBD. Using sustainably sourced HBA and/or HBD components, such as biomaterials, DES can be considered as a green solvent.[2,12−17] The unique properties, environmental friendliness, and flexibility in designing DES have been exploited for their use as electrolytes in electroluminescent materials,[19−21] batteries,[22] and electrochromic devices[18,23,24] and as solvents for circularly polarized light-emitting materials.[25] This study exploits the chirality of sustainable biomaterials to develop circularly polarized light-emitting materials using DES.

Materials that emit circularly polarized light are utilized in a number of applications, including quantum computing,[26,27] circularly polarized organic light-emitting diodes,[28−31] and as probes of the chirality of biomolecules.[32−35] Given the utility and importance, it is not surprising that there has been a recent resurgence in research efforts aimed at developing circularly polarized luminescent materials.[36−41] Circularly polarized luminescence (CPL) is the differential emission of left vs right circularly polarized light. In order to compare CPL emission across systems with different overall emission efficiencies, it is common to use the emission dissymmetry factor, g_{em}, shown in eq 1

$$g_{em} = \frac{2(I_L - I_R)}{I_L + I_R} \quad (1)$$

where I_L and I_R are the emission intensities of left and right circularly polarized light, respectively; $I_L - I_R$ is CPL, and $I_L + I_R$ is total luminescence. Therefore, the value of g_{em} can vary from +2 to −2 giving information about the sign and magnitude of polarization. Because of the unique properties of 4f electrons, the 4f−4f transitions in chiral lanthanide complexes will demonstrate dissymmetry factors, g_{em}, that are typically larger than most organic dyes or transition metals.[42−44] Luminescent lanthanide ions have been exploited

Received: July 16, 2019
Revised: September 9, 2019
Published: September 16, 2019

DOI: 10.1021/acssuschemeng.9b04100
ACS Sustainable Chem. Eng. 2019, 7, 16690−16697

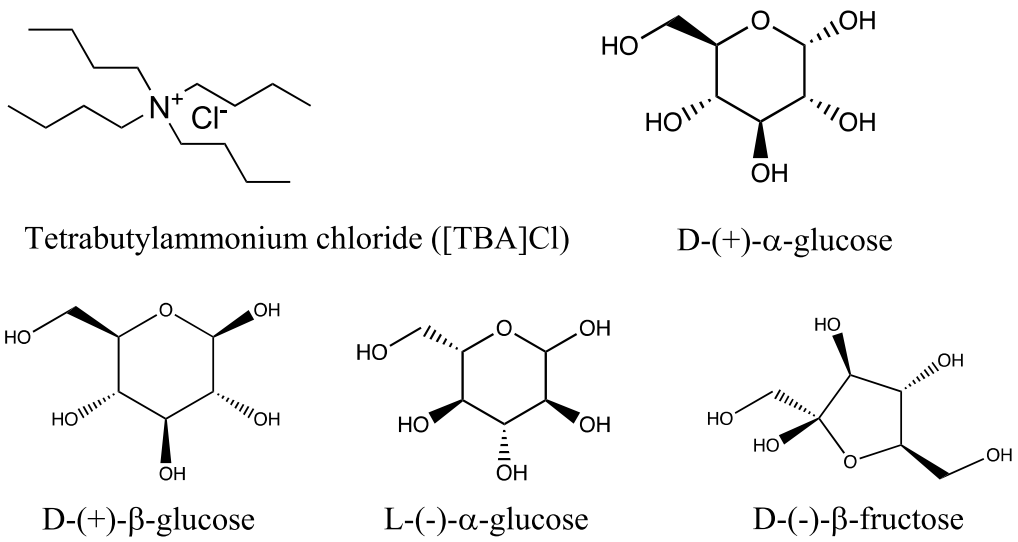

Figure 1. Structures of HBA and HBDs used to form DES used in this study.

for circularly polarized luminescence applications for decades.[45−47]

Using a chiral solvent (or chiral additive), CPL can be induced through a chiral discrimination interaction between the solvent and a racemic mixture of luminescent lanthanide complexes, Λ- and Δ-$Ln(dpa)_3^{3-}$ (where dpa = 2,6-pyridinedicarboxylate dianion, and Ln = Eu or Tb).[48,49] The coordination complex, $Ln(dpa)_3^{3-}$, has left-handed (Λ) or right-handed (Δ) three-bladed propeller arrangement of the ligands about the lanthanide metal, which exists in solution as a racemic mixture of interconverting (Λ ↔ Δ) enantiomers. Previous studies with the racemic $Ln(dpa)_3^{3-}$ complexes dissolved in the chiral IL or DES show that there is a noncovalent chiral interaction that generates a nonracemic population of Λ- vs Δ-$Ln(dpa)_3^{3-}$.[25,50] This chiral discrimination interaction is measured through CPL and quantified by the sign (handedness) and magnitude of g_{em}.

In order to use DES to induce CPL in the $Ln(dpa)_3^{3-}$ complex, HBA and/or HBD must be chiral. Because of the importance of chirality to biology and biochemistry, many of the DES components derived from biomass are chiral, which includes chiral HBDs such as amino acids, fermentation products, and sugars.[11−13,15,51,52] A previous study with amino acid as the chiral HBD and [TBA]Cl and [TBP]Cl (tetrabutylphosphonium chloride) as the HBA demonstrated that chiral DES could induce CPL.[25] This study focuses on the use of monosaccharides, glucose and fructose, as the chiral HBD and [TBA]Cl as the HBA. Figure 1 shows the structures of the [TBA]Cl and fructose used to make DES. L-(−)-glucose is used in this study to compare the impact of overall handedness (L vs D) on the induced CPL. Separate DES are formed with D-(+)-α- and D-(+)-β-glucose as HBD to investigate the impact of orientation at the anomeric carbon on the induced CPL. Only DES with the β anomer of fructose is used for the CPL studies, but the equilibrium mixture of D-(−)-α- and D-(−)-β-fructose is used for the physical property measurements.

Previous studies have shown that glucose and fructose form DES with HBAs, such as choline chloride.[12,13] Since the emitting complexes, $Ln(dpa)_3^{3-}$, are insoluble in monosaccharide DES with choline chloride, [TBA]Cl is utilized as the HBA. Because there are not previous reports of DES formation of fructose or glucose with [TBA]Cl as the HBA, several ratios of [TBA]Cl to glucose (and fructose) are explored to determine which form eutectic mixtures. Eutectic formation is determined by measuring the melting point of the mixture to compare to an ideal solution. The relative polarity is measured for each DES with attention paid to the effect of multiple ratios of [TBA]Cl to D-(+)-α-glucose. The specific rotation is measured for each of DES to ensure that the fructose- and glucose-based DES remain chiral and to measure any isomerization by the monosaccharides.[53,54] The $Ln(dpa)_3^{3-}$ (Eu^{3+} and Tb^{3+}) complexes are dissolved in the glucose- and fructose-based DES to characterize the luminescence, luminescence lifetimes, and the emission of circularly polarized light. The CPL results are interpreted in terms of structural changes in the monosaccharide HBDs, L vs D and α vs β, and with respect to the relative polarity of the DES solvents.

EXPERIMENTAL SECTION

DES Preparation. D-(+)-α-glucose, D-(+)-β-glucose, L-(−)-glucose, D-(−)-fructose, and D-(−)-β-fructose were purchased from Sigma-Aldrich and were used without further purification. [TBA]Cl was purchased from VWR and used without further purification. DES were prepared by mixing the correct mole ratios of hydrogen bond acceptor ([TBA]Cl) with hydrogen bond donor (glucose or fructose) under mild heat (<60 °C). Deep eutectic solvents were prepared in mole ratios of 2:1, 4:1, 6:1, and 8:1 [TBA]Cl:D-(+)-α-glucose, 2:1 [TBA]Cl:D-(−)-fructose (combination of α and β anomers), and [TBA]Cl:D-(−)-β-fructose. Water content of DES was below a measurable level (<0.2%) as measured by Karl Fischer titration (Metroohm 870 KF Titrino Plus).

Physical Measurements. The melting points of DES were measured with a differential scanning calorimeter (DSC), Instrument Specialists Incorporated DSC 550. Samples were prepared by adding 3−10 mg of a DES sample to an aluminum sample pan and lid. DSC was operated with a heating rate of 2 °C/min under a constant flow of helium gas. Densities were determined by determining the mass of DES in a 2.02 mL glass pycnometer. The polarimetry of the monosaccharide-based DES was measured with an Atago AP-300 polarimeter. Polarimetry samples were prepared by dissolving 0.5 g of DES into a 10 mL solution of methanol (or water).

CPL Sample Preparation. All of the starting materials for preparing the $Ln(dpa)_3^{3-}$ samples (where Ln = Eu or Tb), $LnCl_3 \cdot 6H_2O$, and 2,6-pyridinedicarboxylic acid were purchased from Sigma-Aldrich and used without further purification. The complexes were prepared by dissolving $LnCl_3 \cdot 6H_2O$ in water and adding three

DOI: 10.1021/acssuschemeng.9b04100
ACS Sustainable Chem. Eng. 2019, 7, 16690−16697

Table 1. Melting Points and Densities of Monosaccharide DES

	T_M (K)		ρ(g/mL)	T_M (K)
glucose[a]	419	2:1 [TBA]Cl: D-(−)-fructose	1.010	288(2)
fructose[a]	380	3:1 [TBA]Cl: D-(+)-α-glucose	0.960	269(1)
[TBA]Cl[b]	310		ΔH_m = 20.5 kJ/mol	

[a]From ref 55. [b]From ref 56.

equivalents of NaOH to precipitate $Ln(OH)_3$, which was filtered and added to an aqueous solution containing three equivalents of 2,6-pyridinedicarboxylic acid ($dpaH_2$). Three equivalents of tetrabutylammonium hydroxide (TBAOH) were added dropwise to this solution to precipitate $[TBA]_3Ln(dpa)_3$. The water (solvent) was removed by heating under vacuum leaving an oily white solid. Samples were prepared by adding an appropriate mass of $[TBA]_3Ln(dpa)_3$ to approximately 2.0 g of DES to achieve a concentration of 5.0×10^{-4} mol/kg. The sample is stirred under mild heat (<50 °C) for several hours until the complexes dissolved. Emission spectra of the $Ln(dpa)_3^{3-}$ complexes dissolved in DES were recorded on a PerkinElmer LS-55 luminescence spectrometer. Luminescence lifetimes and CPL spectra of the $Ln(dpa)_3^{3-}$ in DES were recorded on a custom-built instrument described previously.[50]

Polarity Measurements. Coumarin-153 was purchased from Exciton laser dyes, and 1-ethyl-4-(methoxycarbonyl)pyridinium iodide (Kosower's salt) was purchased from Sigma-Aldrich. Coumarin samples in the molecular solvents (acetonitrile, methanol, and chloroform) were prepared with a 2−4 μM concentration. The DES samples were prepared by dissolving approximately 1 mg of coumarin in approximately 3 g of DES (approximately 2 mol/kg). Emission spectra of the coumarin samples were recorded on a PerkinElmer LS-55 luminescence spectrometer. Samples were prepared with 0.038 mol/kg Kosower's salt dissolved in DES, and absorption spectra (250−600 nm wavelength range) were recorded with a Cary 60 spectrophotometer. An absorption spectrum of each DES was recorded and used as the baseline.

RESULTS AND DISCUSSION

The melting points and densities determined for 2:1 [TBA]Cl:D-fructose and 3:1 [TBA]Cl:D-(+)-α-glucose are shown in Table 1 along with literature values for the melting points of the pure components.[55,56] Both DES have melting points below room temperature and that of the pure components. Neither a melting point or glass transition was observed for 2:1 (or 1:1) [TBA]Cl:D-(+)-α-glucose DES over the experimental temperature range (253−323 K) of DSC. The observed melting points for 4:1 and 6:1 [TBA]Cl:D-(+)-α-glucose were significantly higher (281 and ∼293 K) than the 3:1 [TBA]Cl:D-(+)-α-glucose. Although this is not close to a complete solid−liquid phase equilibrium evaluation, there is enough data to suggest that the eutectic point is a molar ratio of less than or equal to 2:1 [TBA]Cl:D-(+)-α-glucose. In order to determine if the melting point depression is below that of an ideal solution, the activity coefficient for the major component, [TBA]Cl, of the mixture is determined. The thermodynamics of the solid liquid equilibrium for the mixtures of [TBA]Cl and fructose or glucose can be described using the freezing point depression expression shown in eq 2

$$\ln(\gamma_{TBAC} x_{TBAC}) = \frac{\Delta H_{m,TBAC}}{R}\left(\frac{1}{T_m} - \frac{1}{T}\right) \quad (2)$$

where x_{TBAC} and γ_{TBAC} are the mole fraction and activity coefficients of [TBA]Cl, R is the gas constant, T_m and $\Delta H_{m,TBAC}$ are the melting point and enthalpy of melting of pure [TBA]Cl, and T is the melting point of the mixture. This equation is written assuming that the contribution from the change in heat capacity upon melting ($\Delta_m C_p$) is negligible.[11] Using the melting point and enthalpy of melting from Table 1, the activity coefficient is calculated for each mixture, γ_{TBAC} = 0.825 in 2:1 [TBA]Cl:D-(−)-fructose and γ_{TBAC} = 0.397 in 3:1 [TBA]Cl:D-(+)-α-glucose. Both of these mixtures show negative deviation ($\gamma_{TBAC} < 1$) from ideality, indicating that the interactions (e.g., hydrogen bonding) between [TBA]Cl and glucose (or fructose) are more favorable than interactions within [TBA]Cl alone. The depression of the melting points shown in Table 1 is relatively modest (∼20−40 K) compared to some of the initial choline chloride DES.[6,10] However, the measured activity coefficients show that these [TBA]Cl:D-(−)-fructose and [TBA]Cl:D-(+)-α-glucose mixtures can be classified as deep eutectic solvents.

Polarity. The collection of solvent−solute interactions (e.g., dispersion, hydrogen bonding, . . .), loosely termed as the "polarity" of the solvent, are relevant to the role of DES as a solvent to chiral light-emitting materials. There are several established empirical measures of polarity based on the spectroscopic response of solvatochromatic dyes, including the fluorescent laser dye, coumarin (shown in Figure 2).[57,58]

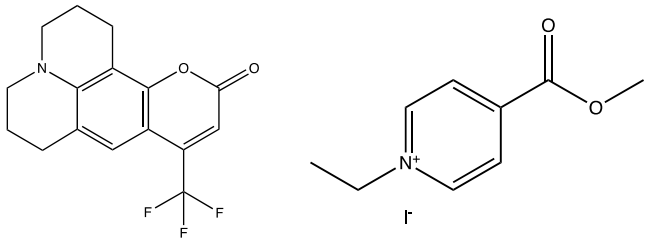

Coumarin 153 Kosower's Salt

Figure 2. Structures of solvatochromatic probes used to empirically measure relative polarity.

Table 2 shows the energy of the maximum emission transition of coumarin dissolved in glucose and fructose DES and several molecular solvents. In order to adapt the energies of coumarin

Table 2. Relative Polarity Data from Solvatochromatic Dye Measurements

DES	E_T (cm^{-1})	E_T^N	Z (kcal/mol)[a]
2:1 [TBA]Cl:D-(+)-α-glucose	20,208	0.471	57
3:1 [TBA]Cl:D-(+)-α-glucose	19,920	0.552	
4:1 [TBA]Cl:D-(+)-α-glucose	19,455	0.667	
6:1 [TBA]Cl:D-(+)-α-glucose	19,380	0.690	
2:1 [TBA]Cl:D-(−)-fructose	19,763	0.588	69
Chloroform	20,387	0.422	
Acetonitrile	19,268	0.719	71[b]
Methanol	18,868	0.825	83[b]

[a]Uncertainty in Z = ± 2 kcal/mol. [b]Z measured in ref 58.

DOI: 10.1021/acssuschemeng.9b04100
ACS Sustainable Chem. Eng. 2019, 7, 16690−16697

into an empirical measure of solvent polarity, the following equation applies

$$E_T^N = \frac{E_T(\text{solvent}) - E_T(\text{cyclohexane})}{E_T(H_2O) - E_T(\text{cyclohexane})} \quad (3)$$

where the transition energy of coumarin is related to the transition energy in cyclohexane (21980 cm^{-1}) and water (18210 cm^{-1}).[57] According to the measure of polarity shown in Table 2, both of the monosaccharide-based DES are moderately polar (i.e., less polar than acetonitrile but more polar than chloroform) at the measured molar ratios of [TBA]Cl to monosaccharide. The E_T^N data also shows that the polarity of 2:1 [TBA]Cl:D-(+)-α-glucose increases as the ratio of [TBA]Cl salt (HBA) increases.

As noted in the literature, the polarity of a solvent is highly dependent upon the nature of the solvatochromatic probe.[59] Because the luminescent lanthanide complexes dissolved in the chiral DES to make chiral light-emitting materials are ionic compounds (salts), it is potentially interesting to empirically measure the polarity using Kosower's salt. The charge transfer transition in Kosower's salt can only happen when the ions are in close proximity, which is a better reflection of the impact of the DES polarity on ionic solutes.[58] Kosower's Z scale is the energy in kcal/mol of the charge transfer transition.[58] Table 2 shows the measured Z value for 2:1 [TBA]Cl:D-(+)-α-glucose vs D-(−)-fructose DES along with the literature Z values for methanol and acetonitrile. Due to the large background absorbance of DES, the uncertainty in the measurement of Z is rather large (±2 kcal/mol). As is the case for coumarin as the solvatochromatic probe, both DES have Z values less (i.e., less polar) than methanol and acetonitrile. Similar to the polarity results from coumarin (Table 2), 2:1 [TBA]Cl:D-(−)-fructose DES is more polar than 2:1 [TBA]Cl:D-(+)-α-glucose.

Optical Rotation. The optical rotations of the glucose- and fructose-based DES are measured to ensure that the optical activity is maintained upon formation of DES. Since both of the monosaccharides anomerize (e.g., $\alpha \leftrightarrow \beta$) in aqueous solution, it is important to determine if there is a structural change of the monosaccharides in DES.[53,54] Table 3 shows the

Table 3. Specific Rotation Measurements for DES

DES	$[\alpha]^a$	monosaccharide	$[\alpha]^b$
2:1 [TBA]Cl:D-(+)-α-glucose	+15	D-(+)-α-glucose	+110
2:1 [TBA]Cl:D-(+)-β-glucose	+23	D-(+)-β-glucose	+19
2:1 [TBA]Cl:D-(−)-fructose	−57	D-(−)-fructose	−92

[a]Measured for 0.5 g in 10 mL of methanol solution. Similar specific rotations were observed in water. [b]From refs 53 and 54.

specific rotation, $[\alpha]$, measured for each the glucose and fructose DES dissolved in methanol along with the specific rotations for the pure monosaccharides. The sign of $[\alpha]$ in DES corresponds to that of glucose and fructose.[53,54] The magnitudes of $[\alpha]$ in Table 3 are determined based on the concentration of DES (0.5 g/10 mL) dissolved in methanol. Compared to the literature magnitudes of glucose and fructose shown in Table 3,[53,54] it is useful to adjust $[\alpha]$ based on the concentration of the monosaccharide only, which results in an approximately 4-fold increase. For example $[\alpha]$ would be ca. −220 for 2:1 [TBA]Cl: D-(−)-fructose, which if D-(−)-fructose was completely dissociated from [TBA]Cl should be much closer to −92. The magnitudes of $[\alpha]$ adjusted for complete dissociation do not match the literature $[\alpha]$ (Table 3) for any of the three DES.

In water, glucose isomerizes to an equilibrium mixture of α and β anomers.[53] While the optical rotation data shown in Table 3 does not exclude the possibility, CPL measurements (Table 5) are inconsistent with DES that contain a mixture of glucose anomers that would result from isomerization. Additionally, 2:1 [TBA]Cl:D-(+)-α-glucose and 2:1 [TBA]-Cl:D-(+)-β-glucose have different $[\alpha]$, whereas glucose isomerizes to the same mixture in water regardless of the starting anomer (α vs β).[53] Overall, the optical rotation data shows that each DES has a unique $[\alpha]$ that is not simply a result of the dissociated monosaccharide in methanol or water. This indicates the persistence of an interaction between [TBA]Cl and fructose (and glucose) even at the low DES concentration of this study.

Luminescence Spectra. The emission spectra and luminescence lifetimes of Eu^{3+} and Tb^{3+} are sensitive to changes in the structure of the $Eu(dpa)_3^{3-}$ and $Tb(dpa)_3^{3-}$ complex. Figure 3 shows the 4f−4f emission spectra of

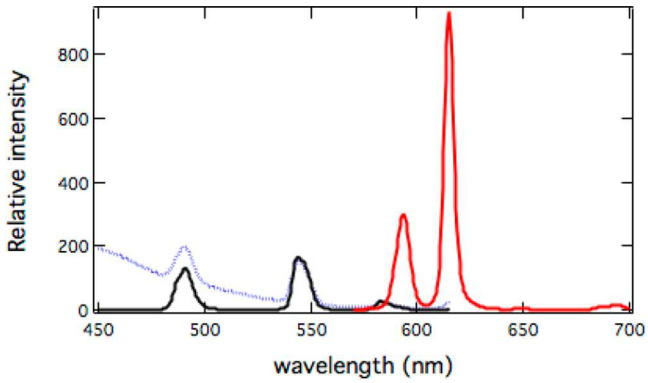

Figure 3. Emission spectra of the $^5D_0 \rightarrow {}^7F_{0-4}$ region of $Eu(dpa)_3^{3-}$ and the $^5D_4 \rightarrow {}^7F_{6-4}$ region of $Tb(dpa)_3^{3-}$ dissolved in 2:1 [TBA]Cl:D-(+)-α-glucose. The dotted blue line is the emission spectrum of $Tb(dpa)_3^{3-}$ without a time delay after excitation, and the solid black ($Tb(dpa)_3^{3-}$) and red ($Eu(dpa)_3^{3-}$) line is the spectrum recorded with a 50 μs delay after excitation. The excitation wavelength is 310 nm.

$Eu(dpa)_3^{3-}$ and $Tb(dpa)_3^{3-}$ dissolved in 2:1 [TBA]Cl:D-(+)-α-glucose DES. There is a small background fluorescence from 2:1 [TBA]Cl:D-(+)-α-glucose, which affects the baseline of the spectra. When the spectrum is recorded after a short time delay (50 μs), the background fluorescence disappears for both the $Eu(dpa)_3^{3-}$ and $Tb(dpa)_3^{3-}$ samples. The spectra shown in Figure 3 have the expected spectral features for $Eu(dpa)_3^{3-}$ and $Tb(dpa)_3^{3-}$.[60,61] For example, there is no symmetry forbidden $^5D_0 \rightarrow {}^7F_0$ transition, and the structure and relative intensities of the $^5D_0 \rightarrow {}^7F_1$ vs $^5D_0 \rightarrow {}^7F_2$ transitions match other $Eu(dpa)_3^{3-}$ systems. The emission spectra of $Eu(dpa)_3^{3-}$ and $Tb(dpa)_3^{3-}$ dissolved in 2:1 [TBA]Cl:D-(−)-fructose are identical in structure to the spectra shown in Figure 3.

The luminescence lifetimes for the $^5D_0$ state of $Eu(dpa)_3^{3-}$ and the $^5D_4$ state of $Tb(dpa)_3^{3-}$ dissolved in DES are shown in Table 4. All of the traces showed monoexponential decay with $Eu(dpa)_3^{3-}$ lifetimes of 2.31−2.36 ms in both DES and a much shorter lifetime, 837 μs, for $Tb(dpa)_3^{3-}$. These lifetimes are similar to those observed in amino acid-based DES[25] and are much longer than the lifetime of $Eu(dpa)_3^{3-}$ and $Tb(dpa)_3^{3-}$

DOI: 10.1021/acssuschemeng.9b04100
ACS Sustainable Chem. Eng. 2019, 7, 16690−16697

Table 4. Measured Luminescence Lifetimes

	2:1 [TBA]Cl:D-(+)-α-glucose	2:1 [TBA]Cl:D-(−)-fructose
$Eu(dpa)_3^{3-}$	2.36 ms	2.31 ms
$Tb(dpa)_3^{3-}$	0.837 ms	n.d.

in water.[62] These measurements confirm that a solvation environment of these DES, like 2:1 [TBA]Cl:L-Glu DES, is not a highly quenching environment for the luminescence of Eu^{3+} and Tb^{3+}. Along with the emission spectra shown in Figure 3, the luminescence and lifetime data suggest that the $Eu(dpa)_3^{3-}$ and $Tb(dpa)_3^{3-}$ coordination environment is stable, and interactions with the DES solvent occur outside of the inner coordination environment of the metals.

CPL Spectra. Figure 4 shows the CPL and total luminescence spectra for the $^5D_0 \rightarrow {}^7F_{1,2}$ region of $Eu(dpa)_3^{3-}$

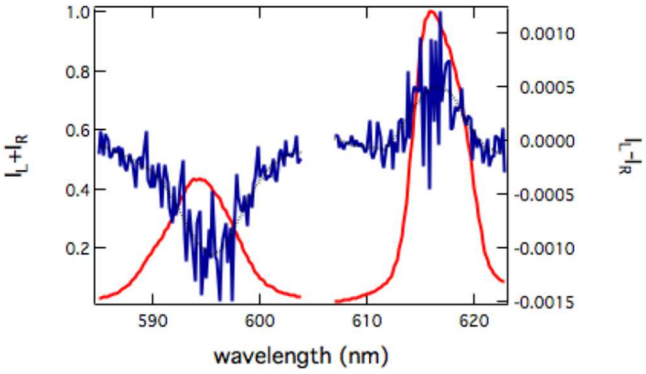

Figure 4. Total luminescence and CPL (noisy) spectra for the $^5D_0 \rightarrow {}^7F_{1,2}$ region of $Eu(dpa)_3^{3-}$ dissolved in 2:1 [TBA]Cl: D-(−)-β-fructose at 303 K. The black dotted lines represent the smoothed CPL spectrum. The intensities of the TL and CPL spectra are normalized.

dissolved in 2:1 [TBA]Cl:D-(−)-β-fructose. The physical property measurements involving [TBA]Cl:D-(−)-fructose, a mixture of the α and β anomers, and samples with $Eu(dpa)_3^{3-}$ dissolved in [TBA]Cl:D-(−)-fructose do show a smaller but nonzero CPL spectrum. However, it is difficult to separate the impact of each anomer on chiral discrimination, and the CPL spectra and analysis focus on [TBA]Cl:D-(−)-β-fructose DES. Figure 4 shows a large negative CPL signal for the magnetic dipole-allowed $^5D_0 \rightarrow {}^7F_1$ transition of $Eu(dpa)_3^{3-}$ at 595.5 nm, and the $^5D_0 \rightarrow {}^7F_2$ transition of $Eu(dpa)_3^{3-}$ at 615 nm shows a positive CPL signal. These CPL transitions are close to the maximum in the total luminescence and opposite in sign to each other, which is consistent with $Eu(dpa)_3^{3-}$ CPL spectra in other systems.[25,50,63] These spectra show that 2:1 [TBA]-Cl:D-(−)-β-fructose DES does enantioselectively perturb the Λ-$Eu(dpa)_3^{3-} \rightarrow$ Δ-$Eu(dpa)_3^{3-}$ racemization equilibrium.

Figure 5 shows the CPL and total luminescence spectra for magnetic dipole allowed $^5D_0 \rightarrow {}^7F_1$ transition of $Eu(dpa)_3^{3-}$ dissolved in 2:1 [TBA]Cl:L-(−)- vs D-(+)-α-glucose. The shape and location of the peaks in the total luminescence spectra are identical for DES with L-(−)- vs D-(+)-α-glucose as HBD. The peaks in the CPL spectra also have identical shapes, locations (595.5 nm), and opposite signs for the L-(−)- vs D-(+)-α-glucose DES. These spectra are consistent with total luminescence and CPL spectra observed for $Eu(dpa)_3^{3-}$ in 2:1 [TBA]Cl:D-(−)-β-fructose (Figure 4). Figure 5 shows that the handedness of α-glucose HBD in DES can be used to control the enantiomeric preference of the

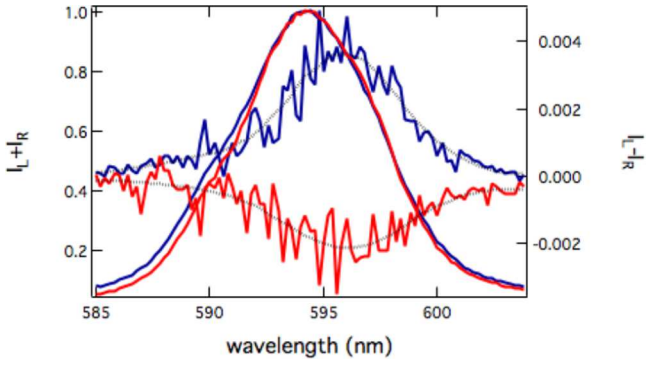

Figure 5. Total luminescence and CPL (noisy) spectra of the $^5D_0 \rightarrow {}^7F_1$ region of $Eu(dpa)_3^{3-}$ dissolved in 2:1 [TBA]Cl:L-(−)- (blue) vs D-(+)-α-glucose (red). The black dotted lines represent the smoothed CPL spectrum. The intensities of the TL and CPL spectra are normalized. The spectra were recorded at 303 K.

perturbation to the racemization equilibrium and thus the polarization of the emitted light. Comparison of 2:1 [TBA]-Cl:D-(+)-glucose (Figure 5) and 2:1 [TBA]Cl:D-(−)-β-fructose (Figure 4) DES show that both produced negative CPL from $Eu(dpa)_3^{3-}$.

In order to demonstrate the effectiveness of the monosaccharide-based DES to produce green chiral light, the CPL spectra of $Tb(dpa)_3^{3-}$ dissolved in [TBA]Cl:D-(+)-α-glucose is measured. The total luminescence and CPL spectra of the magnetic dipole-allowed $^5D_4 \rightarrow {}^7F_5$ transition of $Tb(dpa)_3^{3-}$ in [TBA]Cl:D-(+)-α-glucose is shown in Figure 6. The total

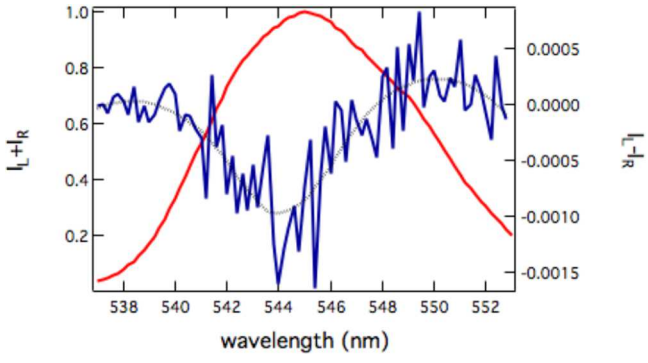

Figure 6. Total luminescence and CPL (noisy) spectra for the $^5D_4 \rightarrow {}^7F_5$ region of $Tb(dpa)_3^{3-}$ dissolved in [TBA]Cl:D-(+)-α-glucose at 303 K. The black dotted lines represent the smoothed CPL spectrum. The intensities of the TL and CPL spectra are normalized.

luminescence shows a broad peak with a maximum at 545 nm and a shoulder transition at 549 nm. The CPL spectrum in Figure 6 shows one negative peak at approximately 544 nm with an emission dissymmetry, $g_{em} = -0.002$. The CPL spectrum does not exactly match that observed for $Tb(dpa)_3^{3-}$ in [TBA]Cl:L-Glu.[25] However, the number of Stark level to Stark level transitions in the $^5D_4 \rightarrow {}^7F_5$ region increases the possibility of interference in the CPL spectrum and also increases the difficulty in interpretation.

DOI: 10.1021/acssuschemeng.9b04100
ACS Sustainable Chem. Eng. 2019, 7, 16690−16697

Emission dissymmetries. The emission dissymmetry factor, g_{em}, is a measure of the degree of polarization of light and the chiral discrimination (on the racemization equilibrium) demonstrated by the DES. Table 5 shows the g_{em} measured for the $^5D_0 \rightarrow {}^7F_1$ transition at 594 nm of $Eu(dpa)_3^{3-}$ dissolved in the monosaccharide-based DES. This includes the g_{em} determined from the spectra shown in Figures 4 and 5 for 2:1 [TBA]Cl:D-(−)-β-fructose (−0.006), 2:1 [TBA]Cl:D-(+)-α-glucose (−0.005), and 2:1 [TBA]Cl:L-(−)-α-glucose (+0.008). The similarity in magnitudes of the g_{em} show that there is not a large difference in the chiral discrimination by fructose- vs glucose-based DES, but the preference can be controlled through choice of L- vs D-glucose as hydrogen bond donor. A previous study assigned $g_{em} > 0$ to an excess of the Λ-$Eu(dpa)_3^{3-}$ enantiomer and $g_{em} < 0$ to an excess of the Δ-$Eu(dpa)_3^{3-}$ enantiomer.[63] Therefore, 2:1 [TBA]Cl:D-(−)-β-fructose and [TBA]Cl:D-(+)-α-glucose DES preference an increase in the population of the Δ-$Eu(dpa)_3^{3-}$ enantiomer, whereas 2:1 [TBA]Cl:L-(−)-α-glucose preferences the Λ enantiomer. Following an analysis previously published, the g_{em} values in Table 5 show a population shift from racemic of less than 1.5%. For example, g_{em} = +0.008 in 2:1 [TBA]Cl:L-(−)-α-glucose represents a shift from 50% to 51.3% of the Λ- $Eu(dpa)_3^{3-}$.[25] Table 5 also includes measured dissymmetries from higher ratios, 4:1 and 6:1, of [TBA]Cl:D-(+)-α-glucose, and DES formed with the β anomer of glucose.

Table 5. Emission Dissymmetry Factors for $Eu(dpa)_3^{3-}$ in Monosaccharide-Based DES

DES	g_{em} (595 nm)[a] $Eu(dpa)_3^{3-}$
2:1 [TBA]Cl:D-(−)-β-fructose	−0.006
2:1 [TBA]Cl:L-(−)-α-glucose	+0.008
2:1 [TBA]Cl:D-(+)-α-glucose	−0.005
4:1 [TBA]Cl:D-(+)-α-glucose	−0.003
6:1 [TBA]Cl:D-(+)-α-glucose	−0.002
2:1 [TBA]Cl:D-(+)-β-glucose	∼0

[a]Uncertainty in the g^{em} is ±0.001 unless otherwise noted. All measurements are at 303 K.

Because [TBA]Cl and glucose form DES at multiple molar ratios, the impact of the molar composition on chiral discrimination is explored. Table 5 shows the emission dissymmetry factors for 2:1, 4:1, and 6:1 [TBA]Cl:D-(+)-α-glucose, and these results show that the higher ratio of D-(+)-glucose has the highest g_{em}. This could be attributed to more D-(+)-α-glucose available to interact with Λ- vs Δ-$Eu(dpa)_3^{3-}$ as the ratio of [TBA]Cl decreases. However, even in 6:1 [TBA]Cl:D-(+)-α-glucose, D-(+)-α-glucose is in significant excess (∼1000×) compared to $Eu(dpa)_3^{3-}$, which makes it unlikely that the D-(+)-α-glucose:$Eu(dpa)_3^{3-}$ ratio is the primary cause of the decrease in g_{em}. Recall that the results in Table 2 show that the polarity of DES increases with the ratio of [TBA]Cl. Since the chiral discrimination by monosaccharide-based DES reflects strong interactions between the chiral DES and $Eu(dpa)_3^{3-}$ solute, solvent polarity must play a role in the chiral discrimination.

The most surprising result shown in Table 5 is the comparison of dissymmetry factors measured in 2:1 [TBA]Cl:D-(+)-α-glucose vs 2:1 [TBA]Cl:D-(+)-β-glucose. As the results show, switching from the α anomer (−0.005) to the β anomer (∼0) of D-glucose completely wipes out the chiral discrimination ability of DES. Figure 1 shows the structures of D-(+)-α-glucose and D-(+)-β-glucose. The only difference is the orientation of the hydroxyl group at the anomeric carbon, but it is clear from these results that this plays an important role in the mechanism of chiral discrimination with Eu-$(dpa)_3^{3-}$.

CONCLUSION

Chiral DES were developed with [TBA]Cl as the HBA, and glucose and fructose as the HBDs. Several ratios of [TBA]Cl to glucose (or fructose) formed clear liquids when mixed, and melting point measurements show that both [TBA]Cl:D-(+)-α-glucose and [TBA]Cl:D-(−)-fructose form DES. Specific rotation measurements show that each DES has optical activity with a sign that is the same as the monosaccharide HBD, but the magnitudes show that there is still some intermolecular interaction between HBA and HBD even dissolved in solvent. The relative polarity of the DES has been measured with a solvatochromatic fluorophore. It is clear that the relative polarity of the DES increases as the ratio of [TBA]Cl increases.

Circularly polarized luminescence was observed from $Eu(dpa)_3^{3-}$ (or $Tb(dpa)_3^{3-}$) dissolved in most of the glucose- and fructose-based DES resulting from noncovalent chiral discrimination by the glucose and fructose DES on the Λ- vs Δ-$Eu(dpa)_3^{3-}$ equilibrium. Comparison of the CPL spectra for $Eu(dpa)_3^{3-}$ in 2:1 [TBA]Cl:L-(−)- vs D-(+)-α-glucose shows that the sign of the CPL (g_{em}) and the sense of chiral discrimination are controlled through choice of the glucose enantiomer as HBD. The sign and magnitude of g_{em} are the same for the D-fructose- vs D-glucose-based DES, which implies an insensitivity to the structure of the monosaccharide. However, comparison of [TBA]Cl:D-(+)-α- vs [TBA]Cl:D-(+)-β-glucose shows that there is no chiral discrimination in the DES where the β anomer of glucose is the HBD. Overall, this study shows that chiral DES made from readily available monosaccharides can be used to induce CPL and make both red (Eu^{3+}) and green (Tb^{3+}) chiral light-emitting materials. As with other physicochemical properties, changes to the HBA:HBD ratio and the structure of the monosaccharide (e.g., α vs β anomer) allows control over the ability of the DES to induce CPL.

ASSOCIATED CONTENT

Supporting Information

The Supporting Information is available free of charge on the ACS Publications website at DOI: 10.1021/acssuschemeng.9b04100.

Densities of varying molar ratios of [TBA]Cl:D-(+)-α-glucose DES, DSC thermograms of 3:1 [TBA]Cl:D-(+)-α-glucose and 2:1 [TBA]Cl:D-(−)-fructose, emission spectra of coumarin dissolved in 2:1−6:1 [TBA]Cl:D-(+)-α-glucose, absorbance spectra of Kosower's salt in 2:1 [TBA]Cl:D-(+)-α-glucose and 2:1 [TBA]Cl:D-(−)-fructose, lifetime traces of $Eu(dpa)_3^{3-}$ dissolved in 2:1 [TBA]Cl:L-(−)-α-glucose and 2:1 [TBA]Cl:D-(−)-fructose, and the $^5D_4$ state of $Tb(dpa)_3^{3-}$ dissolved in 2:1 [TBA]Cl:L-(−)-α-glucose. (PDF)

AUTHOR INFORMATION

Corresponding Author

*E-mail: tahopkin@butler.edu.

DOI: 10.1021/acssuschemeng.9b04100
ACS Sustainable Chem. Eng. 2019, 7, 16690−16697

ORCID

Todd A. Hopkins: 0000-0001-9943-6047

Notes

The authors declare no competing financial interest.

■ ACKNOWLEDGMENTS

The authors would like to acknowledge Matthew Moore and Cole Seager for contributing to the polarity measurements. L.V.E. would like to acknowledge the Butler Program for Undergraduate Research for financial support. This manuscript is based upon work supported by the National Science Foundation under 1800269.

■ REFERENCES

(1) van Osch, D. J.G.P.; Zubeir, L. F.; van den Bruinhorst, A.; Rocha, M. A.A.; Kroon, M. C. Hydrophobic Deep Eutectic Solvents as Water-Immiscible Extractants. *Green Chem.* **2015**, *17*, 4518.

(2) van Osch, D.; Dietz, C. H. J. T.; van Spronsen, J.; Gallucci, F.; van Sint Annaland, M.; Tuinier, R.; Kroon, M. C. A Search for Hydrophobic Deep Eutectic Solvents Based on Natural Components. *ACS Sustainable Chem. Eng.* **2019**, *7*, 2933.

(3) Tang, B.; Zhang, H.; Row, K. H. Application of Deep Eutectic Solvents in the Extraction and Separation of Target Compounds from Various Samples. *J. Sep. Science* **2015**, *38* (6), 1053−1064.

(4) Wang, R.; Sun, D.; Wang, C.; Liu, L.; Li, F.; Tan, Z. Biphasic Recognition Chiral Extraction of Threonine Enantiomers in a Two-Phase System Formed by Hydrophobic and Hydrophilic Deep-Eutectic Solvents. *Sep. Purif. Technol.* **2019**, *215*, 102−107.

(5) An, J.; Trujillo-Rodríguez, M. J.; Pino, V.; Anderson, J. L. Non-Conventional Solvents in Liquid Phase Microextraction and Aqueous Biphasic Systems. *Journal of Chromatography A* **2017**, *1500*, 1−23.

(6) Smith, E. L.; Abbott, A. P.; Ryder, K. S. Deep Eutectic Solvents (DESs) and Their Applications. *Chem. Rev.* **2014**, *114* (21), 11060−11082.

(7) Lima, F.; Dave, M.; Silvestre, A. J. D.; Branco, L. C.; Marrucho, I. M. Concurrent Desulfurization and Denitrogenation of Fuels Using Deep Eutectic Solvents. *ACS Sustainable Chem. Eng.* **2019**, *7* (13), 11341−11349.

(8) Hadj-Kali, M. K.; Mulyono, S.; Hizaddin, H. F.; Wazeer, I.; El-Blidi, L.; Ali, E.; Hashim, M. A.; AlNashef, I. M. Removal of Thiophene from Mixtures with N-Heptane by Selective Extraction Using Deep Eutectic Solvents. *Ind. Eng. Chem. Res.* **2016**, *55* (30), 8415−8423.

(9) Riano, S.; Petranikova, M.; Onghena, B.; Vander Hoogerstraete, T.; Banerjee, D.; Foreman, M. R. S.; Ekberg, C.; Binnemans, K. Separation of Rare Earths and Other Valuable Metals from Deep-Eutectic Solvents: A New Alternative for the Recycling of Used NdFeB Magnets. *RSC Adv.* **2017**, *7* (51), 32100−32113.

(10) Abbott, A. P.; Boothby, D.; Capper, G.; Davies, D. L.; Rasheed, R. K. Deep Eutectic Solvents Formed between Choline Chloride and Carboxylic Acids: Versatile Alternatives to Ionic Liquids. *J. Am. Chem. Soc.* **2004**, *126* (29), 9142−9147.

(11) Crespo, E. A.; Silva, L. P.; Martins, M. A. R.; Fernandez, L.; Ortega, J.; Ferreira, O.; Sadowski, G.; Held, C.; Pinho, S. P.; Coutinho, J. A. P. Characterization and Modeling of the Liquid Phase of Deep Eutectic Solvents Based on Fatty Acids/Alcohols and Choline Chloride. *Ind. Eng. Chem. Res.* **2017**, *56* (42), 12192−12202.

(12) Dai, Y.; van Spronsen, J.; Witkamp, G.-J.; Verpoorte, R.; Choi, Y. H. Natural Deep Eutectic Solvents as New Potential Media for Green Technology. *Anal. Chim. Acta* **2013**, *766*, 61−68.

(13) Hayyan, A.; Mjalli, F. S.; AlNashef, I. M.; Al-Wahaibi, Y. M.; Al-Wahaibi, T.; Hashim, M. A. Glucose-Based Deep Eutectic Solvents: Physical Properties. *J. Mol. Liq.* **2013**, *178*, 137−141.

(14) Li, J.; Xiao, H.; Tang, X.; Zhou, M. Green Carboxylic Acid-Based Deep Eutectic Solvents as Solvents for Extractive Desulfurization. *Energy Fuels* **2016**, *30* (7), 5411−5418.

(15) Castro, V. I. B.; Mano, F.; Reis, R. L.; Paiva, A.; Duarte, A. R. C. Synthesis and Physical and Thermodynamic Properties of Lactic Acid and Malic Acid-Based Natural Deep Eutectic Solvents. *J. Chem. Eng. Data* **2018**, *63* (7), 2548−2556.

(16) Florindo, C.; Branco, L. C.; Marrucho, I. M. Quest for Green-Solvent Design: From Hydrophilic to Hydrophobic (Deep) Eutectic Solvents. *ChemSusChem* **2019**, *12* (8), 1549−1559.

(17) Albler, F.-J.; Bica, K.; Foreman, M. R. S.; Holgersson, S.; Tyumentsev, M. S. A Comparison of Two Methods of Recovering Cobalt from a Deep Eutectic Solvent: Implications for Battery Recycling. *J. Cleaner Prod.* **2017**, *167* (Supplement C), 806−814.

(18) Cruz, H.; Jordão, N.; Branco, L. C. Deep Eutectic Solvents (DESs) as Low-Cost and Green Electrolytes for Electrochromic Devices. *Green Chem.* **2017**, *19* (7), 1653−1658.

(19) Zhu, Z.; Liu, C.; Shi, H.; Jiang, Q.; Xu, J.; Jiang, F.; Xiong, J.; Liu, E. An Effective Approach to Enhanced Thermoelectric Properties of PEDOT:PSS Films by a DES Post-Treatment. *J. Polym. Sci., Part B: Polym. Phys.* **2015**, *53* (12), 885−892.

(20) Qin, H.; Panzer, M. J. Chemically Cross-Linked Poly(2-Hydroxyethyl Methacrylate)-Supported Deep Eutectic Solvent Gel Electrolytes for Eco-Friendly Supercapacitors. *ChemElectroChem* **2017**, *4* (10), 2556−2562.

(21) Jordão, N.; Cruz, H.; Pina, F.; Branco, L. C. Studies of Bipyridinium Ionic Liquids and Deep Eutectic Solvents as Electrolytes for Electrochromic Devices. *Electrochim. Acta* **2018**, *283*, 718−726.

(22) Jiang, P.; Chen, L.; Shao, H.; Huang, S.; Wang, Q.; Su, Y.; Yan, X.; Liang, X.; Zhang, J.; Feng, J.; et al. Methylsulfonylmethane-Based Deep Eutectic Solvent as a New Type of Green Electrolyte for a High-Energy-Density Aqueous Lithium-Ion Battery. *ACS Energy Lett.* **2019**, *4* (6), 1419−1426.

(23) Cruz, H.; Jordão, N.; Amorim, P.; Dionísio, M.; Branco, L. C. Deep Eutectic Solvents as Suitable Electrolytes for Electrochromic Devices. *ACS Sustainable Chem. Eng.* **2018**, *6* (2), 2240−2249.

(24) Rong, K.; Zhang, H.; Zhang, H.; Hu, Y.-Y.; Fang, Y.; Dong, S. Deep Eutectic Solvent with Prussian Blue and Tungsten Oxide for Green and Low-Cost Electrochromic Devices. *ACS Appl. Electron. Mater.* **2019**, *1* (6), 1038−1045.

(25) Wright, C. R.; VandenElzen, L.; Hopkins, T. A. Deep Eutectic Solvents for Induced Circularly Polarized Luminescence. *J. Phys. Chem. B* **2018**, *122* (37), 8730−8737.

(26) Sherson, J. F.; Krauter, H.; Olsson, R. K.; Julsgaard, B.; Hammerer, K.; Cirac, I.; Polzik, E. S. Quantum Teleportation between Light and Matter. *Nature* **2006**, *443* (7111), 557−560.

(27) Bennett, C. H.; DiVincenzo, D. P. Quantum Information and Computation. *Nature* **2000**, *404* (6775), 247−255.

(28) Zhang, X.; Zhang, Y.; Zhang, H.; Quan, Y.; Li, Y.; Cheng, Y.; Ye, S. High Brightness Circularly Polarized Organic Light-Emitting Diodes Based on Nondoped Aggregation-Induced Emission (AIE)-Active Chiral Binaphthyl Emitters. *Org. Lett.* **2019**, *21* (2), 439−443.

(29) Malysheva, E. I.; Dorokhin, M. V.; Demina, P. B.; Zdoroveyshchev, A. V.; Rykov, A. V.; Ved', M. V.; Danilov, Yu. A. Control of Circular Polarization of Electroluminescence in Spin Light-Emitting Diodes Based on InGaAs/GaAs/Δ ⟨Mn⟩ Heterostructures. *Phys. Solid State* **2017**, *59* (11), 2162−2167.

(30) Zinna, F.; Pasini, M.; Galeotti, F.; Botta, C.; Di Bari, L.; Giovanella, U. Design of Lanthanide-Based OLEDs with Remarkable Circularly Polarized Electroluminescence. *Adv. Funct. Mater.* **2017**, *27* (1), 1603719.

(31) Zinna, F.; Giovanella, U.; Bari, L. D. Highly Circularly Polarized Electroluminescence from a Chiral Europium Complex. *Adv. Mater.* **2015**, *27*, 1791−1795.

(32) Neil, E. R.; Fox, M. A.; Pal, R.; Parker, D. Induced Europium CPL for the Selective Signalling of Phosphorylated Amino-Acids and O-Phosphorylated Hexapeptides. *Dalton Trans* **2016**, *45* (20), 8355−8366.

(33) Okutani, K.; Nozaki, K.; Iwamura, M. Specific Chiral Sensing of Amino Acids Using Induced Circularly Polarized Luminescence of Bis(Diimine)Dicarboxylic Acid Europium(III) Complexes. *Inorg. Chem.* **2014**, *53*, 5527.

DOI: 10.1021/acssuschemeng.9b04100
ACS Sustainable Chem. Eng. 2019, 7, 16690−16697

(34) Wu, T.; Průša, J.; Kessler, J.; Dračínský, M.; Valenta, J.; Bouř, P. Detection of Sugars via Chirality Induced in Europium(III) Compounds. *Anal. Chem.* **2016**, *88* (17), 8878−8885.
(35) Jennings, L.; Waters, R. S.; Pal, R.; Parker, D. Induced Europium Circularly Polarized Luminescence Monitors Reversible Drug Binding to Native A1-Acid Glycoprotein. *ChemMedChem* **2017**, *12* (3), 271−277.
(36) Zhao, B.; Pan, K.; Deng, J. Combining Chiral Helical Polymer with Achiral Luminophores for Generating Full-Color, On-Off, and Switchable Circularly Polarized Luminescence. *Macromolecules* **2019**, *52* (1), 376−384.
(37) Jiménez, J.; Cerdán, L.; Moreno, F.; Maroto, B. L.; García-Moreno, I.; Lunkley, J. L.; Muller, G.; de la Moya, S. Chiral Organic Dyes Endowed with Circularly Polarized Laser Emission. *J. Phys. Chem. C* **2017**, *121* (9), 5287−5292.
(38) Nishimura, H.; Tanaka, K.; Morisaki, Y.; Chujo, Y.; Wakamiya, A.; Murata, Y. Oxygen-Bridged Diphenylnaphthylamine as a Scaffold for Full-Color Circularly Polarized Luminescent Materials. *J. Org. Chem.* **2017**, *82* (10), 5242−5249.
(39) Feuillastre, S.; Pauton, M.; Gao, L.; Desmarchelier, A.; Riives, A. J.; Prim, D.; Tondelier, D.; Geffroy, B.; Muller, G.; Clavier, G.; et al. Design and Synthesis of New Circularly Polarized Thermally Activated Delayed Fluorescence Emitters. *J. Am. Chem. Soc.* **2016**, *138* (12), 3990−3993.
(40) Zinna, F.; Arrico, L.; Di Bari, L. Near-Infrared Circularly Polarized Luminescence from Chiral Yb(III)-Diketonates. *Chem. Commun.* **2019**, *55* (46), 6607−6609.
(41) Gorecki, M.; Carpita, L.; Arrico, L.; Zinna, F.; Di Bari, L. Chiroptical Methods in a Wide Wavelength Range for Obtaining Ln3+ Complexes with Circularly Polarized Luminescence of Practical Interest. *Dalton Trans* **2018**, *47* (21), 7166−7177.
(42) Alnoman, R. B.; Rihn, S.; O'Connor, D. C.; Black, F. A.; Costello, B.; Waddell, P. G.; Clegg, W.; Peacock, R. D.; Herrebout, W.; Knight, J. G.; et al. Circularly Polarized Luminescence from Helically Chiral N,N,O,O-Boron-Chelated Dipyrromethenes. *Chem. - Eur. J.* **2016**, *22* (1), 93−96.
(43) Saleh, N.; Srebro, M.; Reynaldo, T.; Vanthuyne, N.; Toupet, L.; Chang, V. Y.; Muller, G.; Williams, J. A. G.; Roussel, C.; Autschbach, J. Enantio-Enriched CPL-Active Helicene-Bipyridine-Rhenium Complexes. *Chem. Commun.* **2015**, *51*, 3754.
(44) Ray, C.; Sánchez-Carnerero, E. M.; Moreno, F.; Maroto, B. L.; Agarrabeitia, A. R.; Ortiz, M. J.; López-Arbeloa, Í.; Bañuelos, J.; Cohovi, K. D.; Lunkley, J. L.; et al. Bis(HaloBODIPYs) with Labile Helicity: Valuable Simple Organic Molecules That Enable Circularly Polarized Luminescence. *Chem. - Eur. J.* **2016**, *22* (26), 8805−8808.
(45) Zinna, F.; Di Bari, L. Lanthanide Circularly Polarized Luminescence: Bases and Applications. *Chirality* **2015**, *27* (1), 1−13.
(46) Carr, R.; Evans, N. H.; Parker, D. Lanthanide Complexes as Chiral Probes Exploiting Circularly Polarized Luminescence. *Chem. Soc. Rev.* **2012**, *41* (23), 7673−7686.
(47) Riehl, J. P.; Richardson, F. S. Circularly Polarized Luminescence Spectroscopy. *Chem. Rev.* **1986**, *86* (1), 1−16.
(48) Muller, G.; Riehl, J. P. Use of Induced Circularly Polarized Luminescence (CPL) from Racemic D-3 Lanthanide Complexes to Determine the Absolute Configuration of Amino Acids. *J. Fluoresc.* **2005**, *15* (4), 553−558.
(49) Yan, F.; Brittain, H. G. Pfeiffer Effect Optical Activity Developed in Lanthanide Tris(Pyridine-2,6-Dicarboxylate) Complexes by Chiral Tartrate Substrates. *Polyhedron* **1982**, *1* (2), 195−199.
(50) Kroupa, D. M.; Brown, C. J.; Heckman, L. M.; Hopkins, T. A. Chiroptical Study of Chiral Discrimination by Amino Acid Based Ionic Liquids. *J. Phys. Chem. B* **2012**, *116* (16), 4952−4958.
(51) Mjalli, F. S. Novel Amino Acids Based Ionic Liquids Analogues: Acidic and Basic Amino Acids. *J. Taiwan Inst. Chem. Eng.* **2016**, *61*, 64−74.
(52) Zhao, B.-Y.; Xu, P.; Yang, F.-X.; Wu, H.; Zong, M.-H.; Lou, W.-Y. Biocompatible Deep Eutectic Solvents Based on Choline Chloride: Characterization and Application to the Extraction of Rutin from Sophora Japonica. *ACS Sustainable Chem. Eng.* **2015**, *3* (11), 2746−2755.
(53) Hudson, C. S.; Dale, J. K. STUDIES ON THE FORMS OF D-GLUCOSE AND THEIR MUTAROTATION. *J. Am. Chem. Soc.* **1917**, *39* (2), 320−328.
(54) Tsuzuki, Y.; Yamazaki, J.; Kagami, K. The Specific Rotation of Fructose. *J. Am. Chem. Soc.* **1950**, *72* (3), 1071−1073.
(55) Hurtta, M.; Pitkänen, I.; Knuutinen, J. Melting Behaviour of D-Sucrose, d-Glucose and d-Fructose. *Carbohydr. Res.* **2004**, *339* (13), 2267−2273.
(56) Coker, T. G.; Ambrose, J.; Janz, G. J. Fusion Properties of Some Ionic Quaternary Ammonium Compounds. *J. Am. Chem. Soc.* **1970**, *92* (18), 5293−5297.
(57) Reichardt, C. Solvatochromic Dyes as Solvent Polarity Indicators. *Chem. Rev.* **1994**, *94* (8), 2319−2358.
(58) Kosower, E. M. The Effect of Solvent on Spectra. I. A New Empirical Measure of Solvent Polarity: Z-Values. *J. Am. Chem. Soc.* **1958**, *80* (13), 3253−3260.
(59) Florindo, C.; McIntosh, A. J. S.; Welton, T.; Branco, L. C.; Marrucho, I. M. A Closer Look into Deep Eutectic Solvents: Exploring Intermolecular Interactions Using Solvatochromic Probes. *Phys. Chem. Chem. Phys.* **2018**, *20* (1), 206−213.
(60) Hopkins, T. A.; Bolender, J. P.; Metcalf, D. H.; Richardson, F. S. Polarized Optical Absorption and Emission Spectra and the Electronic Energy-Level Structure of Tb(Dpa)33- Complexes in Na3[Yb0.95Tb0.05(Dpa)3]·NaClO4·10H2O. *Inorg. Chem.* **1996**, *35* (18), 5356−5362.
(61) Binnemans, K. Interpretation of Europium(III) Spectra. *Coord. Chem. Rev.* **2015**, *295*, 1−45.
(62) Aebischer, A.; Gumy, F.; Bünzli, J.-C. G. Intrinsic Quantum Yields and Radiative Lifetimes of Lanthanide Tris(Dipicolinates). *Phys. Chem. Chem. Phys.* **2009**, *11* (9), 1346−1353.
(63) Coruh, N.; Hilmes, G. L.; Riehl, J. P. Use of the Pfeiffer Effect to Probe the Optical Activity of Europium(III) Complexes with 2,6-Pyridinedicarboxylate. *Inorg. Chem.* **1988**, *27* (20), 3647−3651.

DOI: 10.1021/acssuschemeng.9b04100
ACS Sustainable Chem. Eng. 2019, 7, 16690−16697